

[7] Analysis of Stress Intensity Factor and Crack Propagation for Alloy X-750 Pressure Vessel with a Blunting Crack

E. Mahdavi^{1,a}, Mahmoud Mosavi Mashhadi^{2,b}, M. Amidpour^{1,c}

¹Department of Mechanical Engineering,
K.N. Toosi University of Technology,
Tehran,
Iran

²Department of Mechanical Engineering,
University of Tehran,
Tehran,
Iran

^aehsanmeasam@gmail.com, ^bmmosavi@ut.ac.ir, ^camidpour@kntu.ac.ir

Keywords: Crack Growth, FEM, Pressure Vessel, Stress Intensity Factor

Abstract

It is well known that the crack growth rate fatigue and stress corrosion cracking can be approximated by a power function of the stress intensity factor. In this study, stress intensity factor for elliptical crack under the uniform tension in linear elastic fracture mechanics (LEFM) is investigated therefore for this purpose, a pressure vessel modeled by finite element. A crack modeled on the pressure vessel and then the stress intensity factor for crack propagation in different methods is evaluated. Finite element analysis calculates stress intensity factor in the values of the J-integral are based on the stress intensity factors, JK, and by evaluating the contour integral directly, JA. The stability of crack growth is considered so the ductile crack extension is determined by pursuing the equilibrium between loading and crack resistance. Using especial method of meshing caused to have accurate results. This method causes to decrease run time and considerable accuracy. Then stress intensity factor is calculated for different position of the crack such as crack front and then compared to each other.

Introduction

Hydrogen embrittlement and brittle fracture of materials are occurred by hydrogen diffusion which is important phenomenon. Bockris et. al. [1] discussed about the effects of hydrogen on various metals and also use of special metals which tolerate these effects. So, improvement of industry made more familiar the man with using high strength steel and application of it [2]. Yokobori et. al. [3] suggested that diffusion occurs when there are gradient of concentration and stress as driving force. Moreover, the stress is also affected around the crack tip. Therefore, it should be constructed a physical model in order to solve coupled mass diffusion with stress to predict the treatment of crack growth. As a result, coupled mass diffusion with stress phenomena occurred by hydrogen diffusion causes some problems for materials like, embrittlement, degradation, crack assisting and finally fast fracture and consequently, material will be failed. Krupp et al. [4] proposed a model for describing of hydrogen embrittlement. It said that while hydrogen contacts with surface of a metal, it needs energy to diffuse and cleavages of micro structure of the metal. Indeed, molecule of hydrogen is big enough not to be able enter the metal and puts itself between the molecules and atoms of the metal. In this process, by chemical reactions the molecule of hydrogen is split into two atoms because of that an amount of energy released to help it to diffuse in the metal's surface Fig.1. After, it is occurred, lines of defects are created and caused to accumulate large amount of atoms of hydrogen in these lines. So, by piling up them, molecules of hydrogen are constructed and consequently stress is produced. Symons [5] implemented properties of metal such as ductility changed into brittle happened called

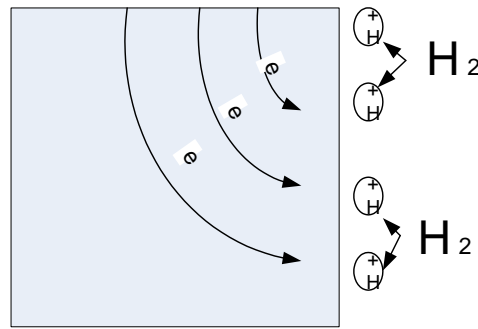


Figure 1
Hydrogen diffusion at the surface of a metal

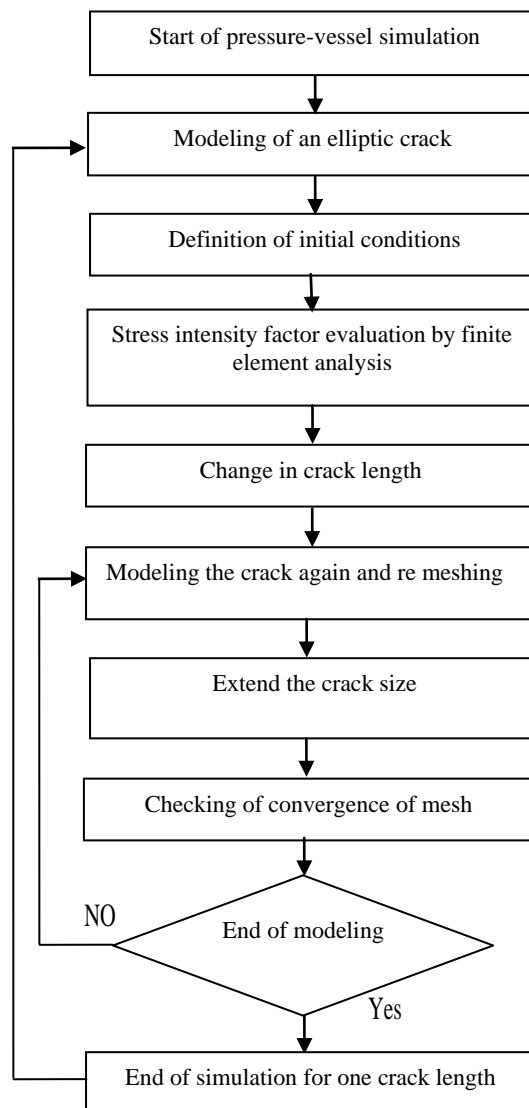


Figure 2
Procedure for crack-growth simulation

degradation. Degradation of mechanical properties is the other effect of hydrogen upon metals. Simultaneously, diffusing of hydrogen and degradation of properties, crack starts growing until complete failure of whole material. So, hydrogen can facilitate crack growing that occurs in either of two ways, one is by a strain-controlled mechanism and the other one is by stress-controlled

decohesion [6]. In fact, if hydrogen attacks at low temperature and decreasing of fracture toughness is happened because of degradation, absolutely fast fracture will be gone to happen [7, 8].

As a result, science of materials and profound mechanical studying of a micro structure in experimental method illustrate the procedure and mechanism of diffusion, degradation, and embrittlement and fracture to some extent but not completely [9, 10]. For this purpose, different models have been proposed by different researchers to describe this mechanism more complete and accurate. There were three basic models that introduced by Zapff-Tetelman, Petch and Troiono. In addition, Zapff-Tetelman's model considered only hydrogen diffusion. But, this model could not see the stress parameter. Petch's model just proposed effects of fracture energy on hydrogen diffusion phenomena. But there was some defects like incomplete model involved diffusion. Troiono's model predicted interatomic band and focused on micro scales reactions between hydrogen atoms which diffused. However, it was unable to foresee and make judgment for macro scales and a coupled mass diffusion with stress in a metal [11]. Another model defined the role of strain rate at a crack tip consisting a cylinder subjected to tension is parallel to cylinder axes [12]. Liu [13] proposed a model for elastic field on crack tip. Li et al. [14] considered this problem as independent system between H and C without metal components. Really, he presented a thermodynamic analysis of metal-hydrogen model to find a relation between concentration and stress. But the biggest problem was related not to be able to describe fracture mechanics. A model has been developed describing both the microscopic and macroscopic features of embrittlement due to dissolving or internal hydrogen [15]. These are models which described above converged to find a more reliable solution to predict material's behavior during coupled mass diffusion with stress and answer certainly and surely to many questions about mass diffusion. According to the problems have been occurred due to mass diffusion phenomena in industry especially for pressure vessels; encourage us to research in this field. One of the main concerning during an operation of a pressure vessel is susceptibility of it to an embrittlement. To have a required safety margin against a fracture, should be tried with ASME Cod Section 3 and 4 [16]. There are two important points to evaluate the condition of a pressure vessel for operating. First is fracture toughness and second is the ratio of stress intensity factor to fracture toughness [17]. Diffusion occurs when there are gradient of concentration and stress as driving forces [18, 19]. The effects of hydrogen on various metals and use of metals which are well to tolerate them are very important point [20]. So, it is should be constructed a physical model in order to solve a diffusion equation to predict the treatment of mass diffusion and stress. In this study, for having more accurate analysis and perfect evaluation of the coupled mass diffusion with stress equation, it is essential to have a model can describe and illustrate what happen during mass diffusion and how efficiently it confirms two main points such as accumulating of hydrogen concentration always is happened near the crack tip and maximum hydrostatic stress is occurred there. If one model is associated with these two main characteristics, it is possible to accept it as a reliable model for analysis of a coupled mass diffusion with stress equation. Therefore, a model for a pressure vessel exposed to mass diffusion is made and coupled mass diffusion with stress is investigated how hydrogen embrittlement can influence on the fracture toughness of its material by FEM. In addition, mass diffusion is described by Fick's law. There are two driving forces, the first one is gradient of concentration and the second is gradient of stress. So, these two gradients give us the flux of coupled mass diffusion with stress. This formulation is the extended Fick's law introduced by Sofronis [21]. Furthermore, the evaluation is done in LEFM.

FEM method for simulation

ABAQUS v.7.1 soft ware is employed to predict it because of its capacity in analysis of stress. Fig. 2 shows crack simulation and its procedure.

Modeling of a pressure vessel

The simulation of the problem which involved in items as follows:

Geometrical simulation

A pressure vessel is simulated by finite element in Fig. 3. In this figure, the geometrical measurements are defined. This pressure vessel involves an elliptical crack. Only 1/8 of the pressure vessel is simulated.

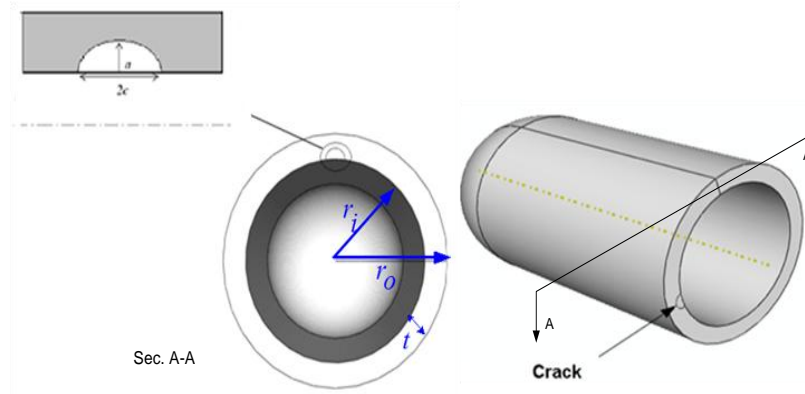


Figure 3
Schematic of a pressure vessel with an elliptical crack

In Fig. 4, the geometrical measurements are defined.

Sizes of geometric: $L1=2300$ mm, $L2=250$ mm. $Ri=250$ mm, $t=20$ mm, $ri=250$ mm

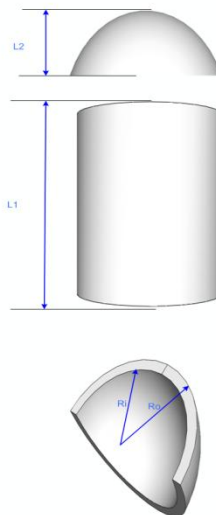
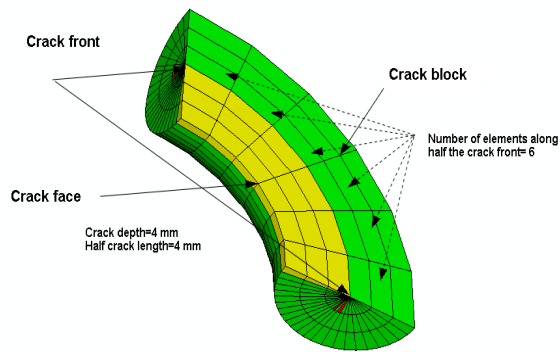


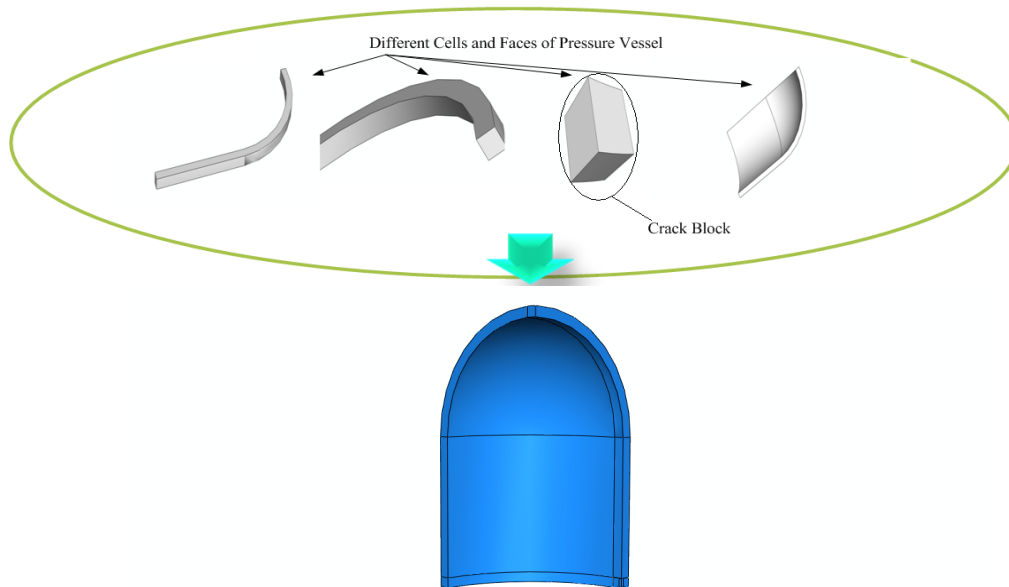
Figure 4
Schematic view of various parts of a pressure vessel

Also, Fig. 5 illustrates singular elements which are used around the crack front. The basic concept of these elements is that they introduce the solution dominated by the singularity at the crack front. Moreover, Fig.5 shows different parts of the crack such as crack face, crack front and crack block.

**Figure 5**

Schematic of a crack with three parts and singularity of the crack front

For more accuracy in crack simulation, many different partitions are employed, Fig. 6.

**Figure 6**

Various partitions for a pressure vessel

Definition of material property

In the crack simulation, a pressure vessel with a crack molded exposed to 0.34 MPa. Alloy X-750, the material is applicable for building a pressure vessel. The material used in this paper was heated treated to the HTH condition. The HTH condition consists of a solution anneal at 1094°C for 1-2 h with a rapid air cool followed by aging at 704°C for 20 h. The chemical analysis is shown in table 1. Material properties like yield stress, elastic modulus and density are given by Table 2 [5].

Table 1
Chemical analysis (wt%)

Ni	Cr	Nb	Ti	Al	Fe	Co
71.17	15.46	1.00	2.67	0.76	8.33	0.072

Table 2
Mechanical properties of Alloy X-750 at 25°C

Temperature (K)	Yield strength (MPa)	Young's modulus (GPa)	Poisson ratio	Density (g.cm ⁻³)
298	850	213.7	0.3	8.28

Using the tie constraint technique

In order to decrease run time, allowing variations in element shape and element interpolation would require tie constraints between varying regions. This technique can help decreasing the run time by refine meshing. The concept of this technique consists of making size of mesh changed everywhere is necessary.

So, for having accurate results in studied model, the crack block cell should have the smallest mesh of all cells of the pressure vessel because this makes results more precise. For this purpose, the model is separated into two parts. One part is crack block and the other part is the rest of the pressure vessel. So, it tried to make two parts constrain together to act as one part. Precisely, it is useful to use tie constraint technique.

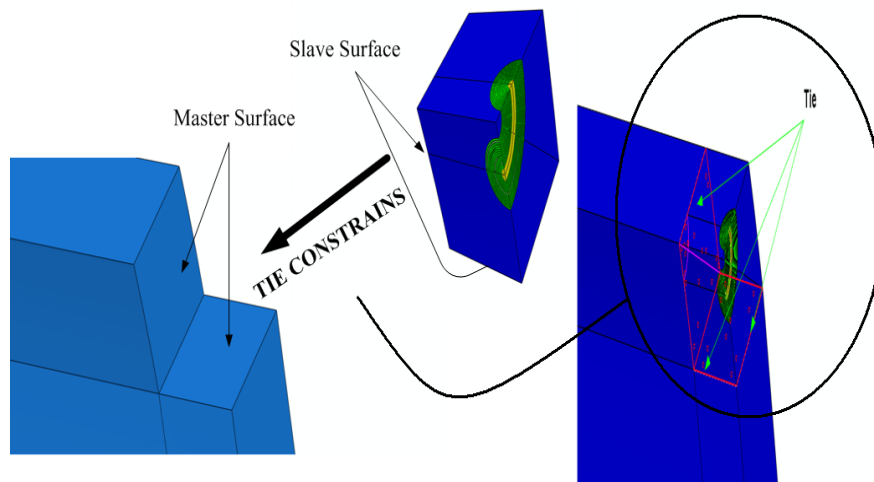


Figure 7

Tie constraint technique used to tie the crack block to the rest of the pressure vessel

According to the figure, the master surface, which is the surface of the larger part and slave surface, is smaller part. Fig. 7 shows the schematic of tie constrain technique to make meshes of the crack block small to obtain accurate results.

Stress analysis

Finite element can be able to evaluate stress analysis in CAE (Complete Abaqus Environment). In this analysis, one modeled pressure vessel with an elliptical crack subjected to inner pressure is analyzed. As a result, contours of stress are created near the crack front.

Boundary conditions for stress analysis

The axisymmetrical model allows 1/8 of the pressure vessel to be modeled. This pressure vessel is subjected to an inside pressure of 0.34 MPa and its faces are restricted according to Fig. 8.

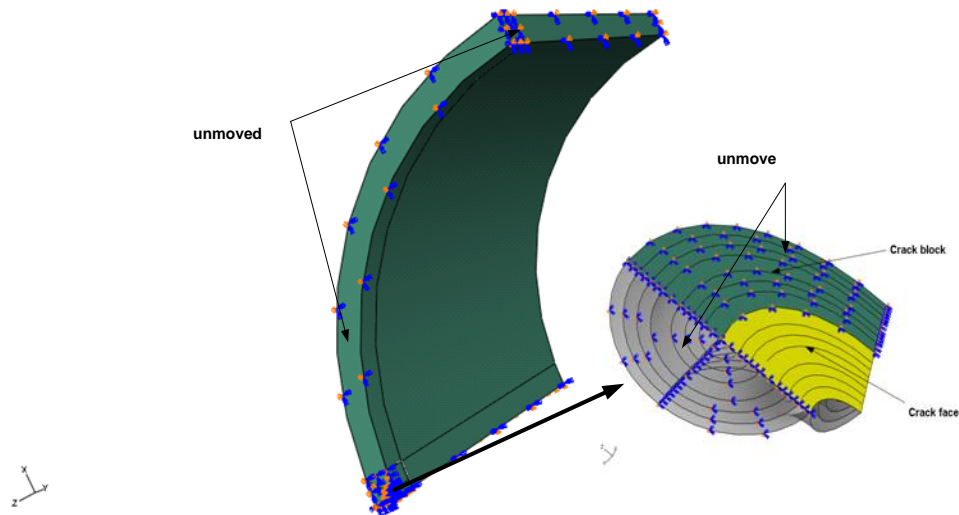


Figure 8
Schematic of 1/8 pressure vessel with boundary conditions

Using suitable elements and property meshing

In the case of changing crack length, the nodes are easily shifted to the new position. Especial mesh technique used to evaluate as well. For the crack front, singular element like wedge and for the block crack used structure mesh. To have a good agreement between cells, the rest of the pressure vessel has sweep technique. Moreover, the finite element mesh consisted of 22715 nodes and 15992 elements. Finer mesh used near the crack tip to enhance accuracy. Two different kinds of element are used for modeling and analysis such as structure element (C3D20R) and wedge element (C3D15R). Elements are used in crack block and for showing singularity at crack front, the wedge elements are used. Shapes of these elements are found in Fig. 9.

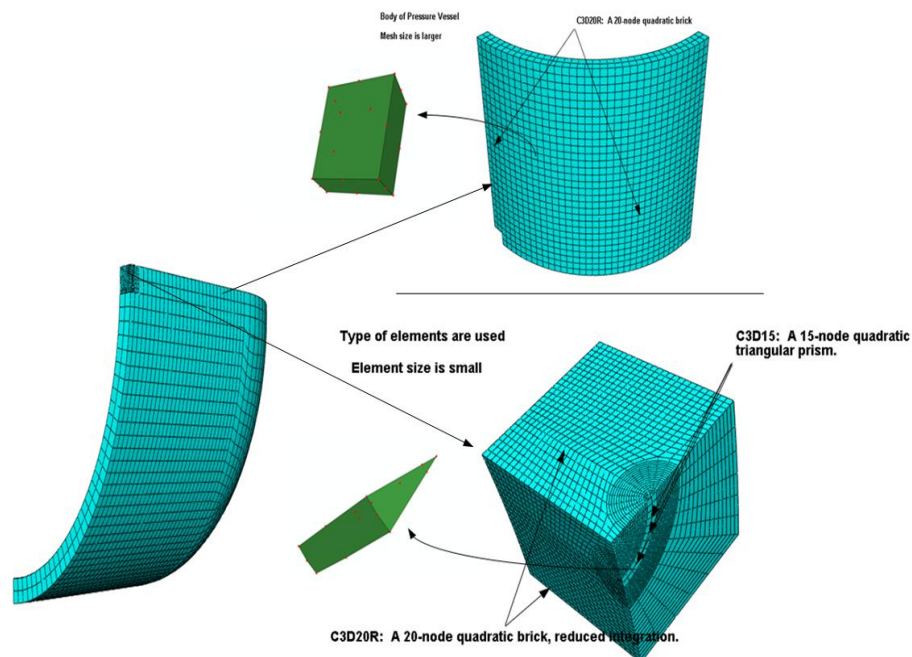


Figure 9
Shape of two kinds of elements: structure element and wedge element

Stress intensity factor evaluation

A novel fracture mechanics technique has been employed for the determination of crack growth as a function of stress intensity factor using pressure vessel with a blunting crack. It is employed different contours around the crack tip to calculate the release energy while crack is growing. The method for crack growth modeling is change in the crack length and calculation of J-integral for each path around the crack tip. For this purpose, different crack length is considered. According to Ref. [22], the stress intensity factor for a crack subjected to uniform tension is as follow:

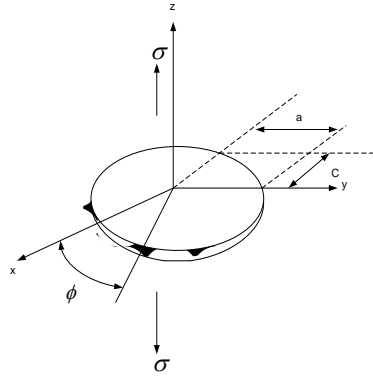


Figure 10
Stress intensity factor for a crack subjected to uniform tension

$$K_I = \frac{\sigma}{E(K)} \left(\frac{c}{a} \right)^{0.5} (a^2 \sin^2 \Phi + b^2 \cos^2 \Phi)$$

$$K = \left(1 - \left(\frac{c}{a} \right)^2 \right)^{0.5} \quad (1)$$

In ABAQUS, the J-integral has a close relationship with the energy release associated with the crack growth. Also, stress intensity factors relates to the energy release rate. The stress intensity factor is calculated for both crack tip and crack front. The J-integral is defined in terms of the energy release rate associated with crack growth. For a virtual crack advance $\lambda(s)$ in the plane of a three-dimensional fracture, the energy release rate is given by

$$J = \int \lambda(s) n \cdot H \cdot q dA$$

Where dA is a surface element along a vanishing small tubular surface enclosing the crack tip or crack line, n is the outward normal to dA , and q is local direction of virtual crack extension. H is given by

$$H = \left(W I - \sigma \cdot \frac{\partial u}{\partial x} \right)$$

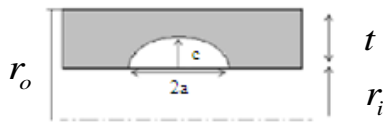
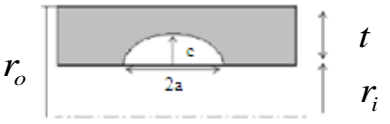
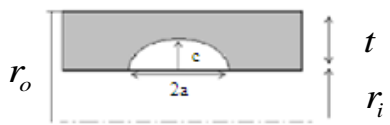
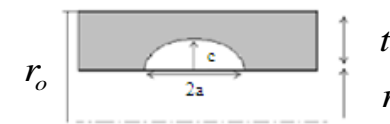
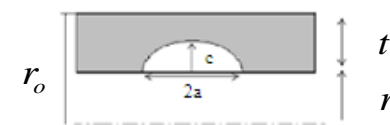
For the elastic material behavior W is the elastic strain energy, for elasto-viscoplastic material behavior W is defined as the elastic strain energy plus the plastic dissipation.

FEM Results and Discussion

Calculation of stress intensity factor and distribution of stress

Different crack lengths are modeled in order to obtain distribution of stress and then evaluate stress intensity factor for deepest point and corner point. The different crack lengths are shown in table 3.

Table 3
Various crack geometries and their dimensions

Geometry	Dimensions
	t=20 mm r _i =250 mm c=4 mm a=4.1 mm
	t=20 mm r _i =250 mm c=4 mm a=4.2 mm
	t=20 mm r _i =250 mm c=4 mm a=4.3 mm
	t=20 mm r _i =250 mm c=4 mm a=4.4 mm
	t=20 mm r _i =250 mm c=4 mm a=4.5 mm

Evaluation of stress intensity factor for elliptical crack by using handbook (Eq. 1)

This study illustrates the changes of stress intensity factor which is obtained by using Eq. 1 and also shown effect of crack length and position of contours on stress intensity factor.

According to table 4, the crack length is 4 mm and crack depth is 4mm. then the crack length is grown from 4 mm to 4.5 mm. In addition, K and K_I are calculated by using Eq. 1.

Table 4
Value of stress intensity factor evaluated from handbook (Eq. 1) for crack tip, $\varphi = 0^\circ$

<i>Crack length a (mm)</i>	<i>Crack depth c(mm)</i>	<i>K</i>	<i>σ (MPa)</i>	<i>E (GPa)</i>	<i>K_I (MPa√m)</i>
4.1	4	0.219512	0.34	213.7	0.114544
4.2	4	0.304911	0.34	213.7	0.081476
4.3	4	0.366971	0.34	213.7	0.066905
4.4	4	0.416598	0.34	213.7	0.058261
4.5	4	0.458123	0.34	213.7	0.052389

Similar to calculation in table 5, this is done for crack front $\varphi = 45^\circ$ and $\varphi = 90^\circ$. These evaluations are given in table 5 and table 6.

Table 5
Value of stress intensity factor evaluated from handbook for crack tip, $\varphi = 45^\circ$

<i>Crack length a (mm)</i>	<i>Crack depth c(mm)</i>	<i>K</i>	<i>σ (MPa)</i>	<i>E (GPa)</i>	<i>K_I (MPa√m)</i>
4.1	4	0.219512	0.34	213.7	0.164421
4.2	4	0.304911	0.34	213.7	0.119912
4.3	4	0.366971	0.34	213.7	0.100956
4.4	4	0.416598	0.34	213.7	0.09013
4.5	4	0.458123	0.34	213.7	0.083085

Table 6
Value of stress intensity factor evaluated from handbook for crack tip, $\varphi = 90^\circ$

<i>Crack length a (mm)</i>	<i>Crack depth c(mm)</i>	<i>K</i>	<i>σ (MPa)</i>	<i>E (GPa)</i>	<i>K_I (MPa√m)</i>
4.1	4	0.219512	0.34	213.7	0.120343
4.2	4	0.304911	0.34	213.7	0.089827
4.3	4	0.366971	0.34	213.7	0.077317
4.4	4	0.416598	0.34	213.7	0.070496
4.5	4	0.458123	0.34	213.7	0.066304

Using finite elements to evaluate stress intensity factor

In This paper, evaluating contour integrals for axisymmetrical and LEFM model are done. As you know that J-integral has closed relation to energy release associated with the crack growth. Also, stress intensity factors relates to the energy release rate. The values of the J-integral are based on the stress intensity factors, JK, and by evaluating the contour integral directly, JA. The table list values for contour 2 through contour 4. In addition, three positions called corner point which is located in $\varphi = 90^\circ$, deepest point which is located in $\varphi = 0^\circ$, and the point is located between them whose situation is in $\varphi = 45^\circ$. Fig. 11 illustrates positions of deepest and corner point.

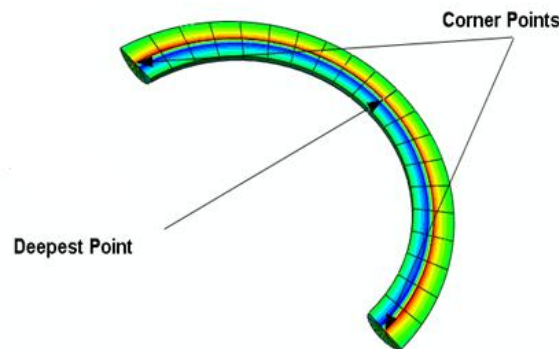


Figure 11
Position of corner point and deepest point in the crack for stress analysis

The stress intensity factor is defined by J-integral around the crack tip trough using different contours which are shown in Fig. 12. Different crack lengths from 4 to 4.5 mm are studied and stress intensity factor is gained for each crack length for different position on crack face. Fig. 11 shows different positions on crack front and three positions according to Fig. 12; $\varphi = 0^\circ, 45^\circ, 90^\circ$.

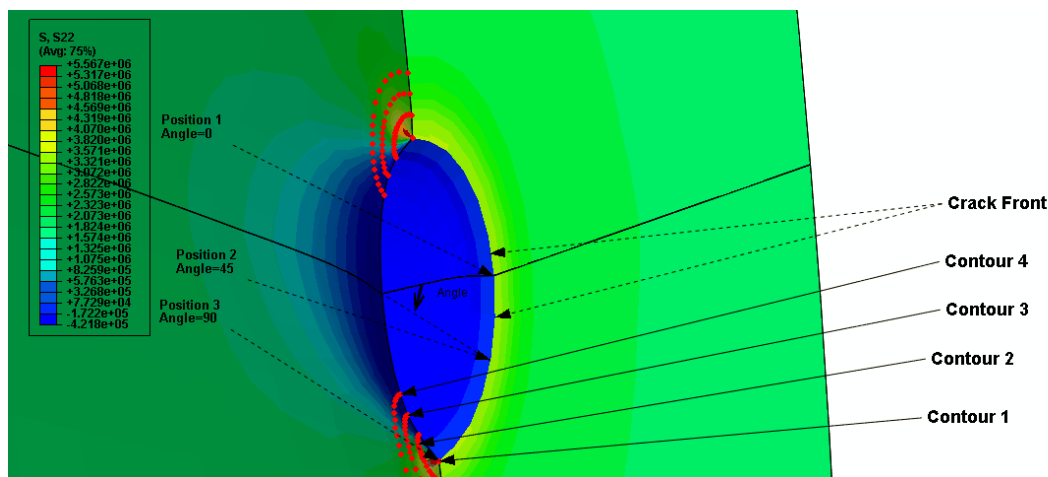


Figure 12
Using various contours and positions to calculate stress intensity factor

Results from the first contour are not used because the first one is influenced by singularity. So, J-integral for each contour is calculated (JA) and the large deviation for JK versus JA is expected because the method of calculating contour integral directly is less sensitive to numerical precision than calculating contour integral from stress intensity factor. The first step is the evaluation of JA, the second step is dealing with JK and the next will be to compare these results with the values of the stress intensity factor obtained from tables 4, 5 and 6 discussed above.

Evaluation of J-integral are based upon contour integral directly (JA)

JA is the first method of calculation of J-integral. Therefore, the first evaluation is related to crack length 4.1 mm. Moreover, hydrogen pressure is 0.34 MPa. As a result, the same method has been done for the other crack length. All results are shown in table 7. In this table, the average value of three contours is evaluated and separated for each crack length.

Table 7
Value of energy rate for various contours

<i>Crack length (mm)</i>	<i>energy release rate for contour 2</i>	<i>energy release rate for contour 3</i>	<i>energy release rate for contour 4</i>	<i>Average of energy release rate ($\times 10^3$)</i>
4.1	1.514	1.423	1.36	1.445
4.2	1.559	1.463	1.398	1.473
4.3	1.566	1.456	1.388	1.47
4.4	1.632	1.542	1.410	1.528
4.5	1.673	1.567	1.496	1.578

Evaluation of J-integral based upon the stress intensity factor (JK)

Finite element is employed again to calculate stress intensity factor but in different method, JK. For this purpose, three contours are considered from 2 to 5 what were mentioned above. According to Fig. 13, the contours in different positions of crack front are considered to evaluate and compare the value of stress intensity factor which are obtained by using JK method. The results are put in table 8. Besides, the accuracy of the JK method is evaluated in table and errors are very small and ignorable.

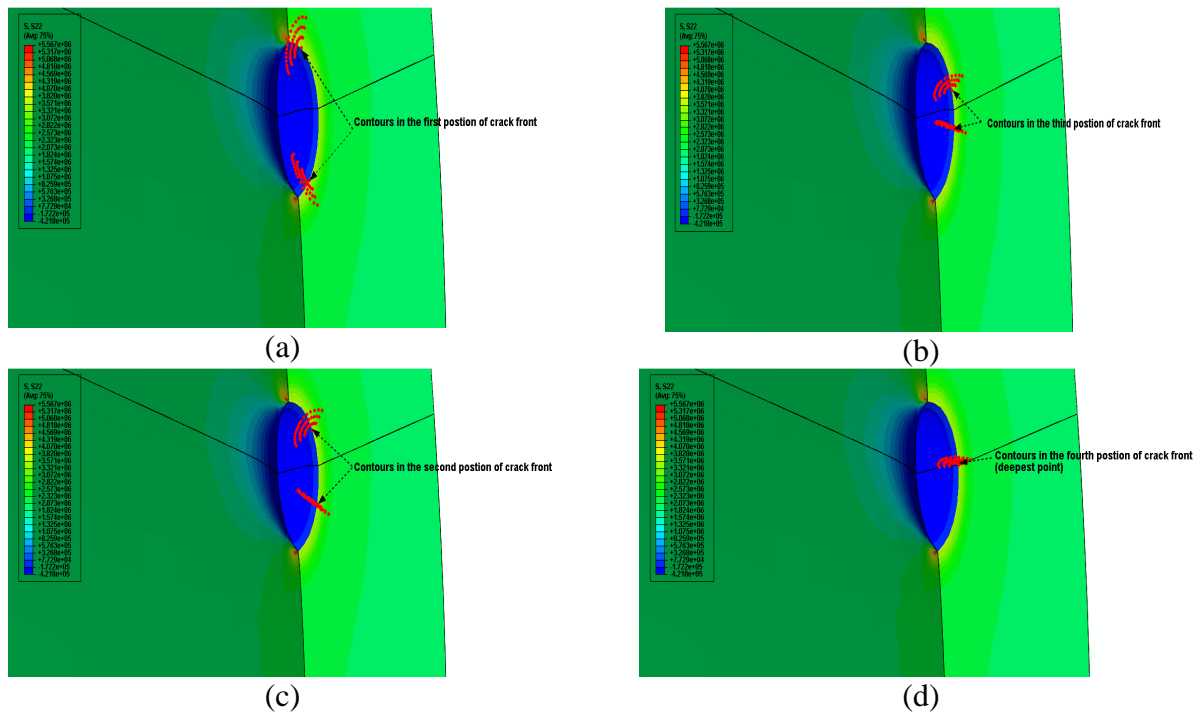


Figure 13
Calculation of JK by using FEM for various positions on the crack front,
a) first position, b) second position, c) third position and d) fourth position

Table 8
Calculation of J-integral and stress intensity factor for a=4.1 mm by finite elements

<i>Crack length=4.1 mm, first position</i>	<i>contour 2</i>	<i>contour 3</i>	<i>contour 4</i>	<i>contour 5</i>	<i>average</i>
JK	9.827	19.57	31.86	46.4	26.91
K_I(Pa√m)	1.52 E+06	2.144 E+06	2.735 E+06	3.3 E+06	2.425E+06
<i>Crack length=4.1 mm, second position</i>	<i>contour 2</i>	<i>contour 3</i>	<i>contour 4</i>	<i>contour 5</i>	<i>average</i>
JK	7.287	17.55	34.29	58.19	29.33
K_I(Pa√m)	1.308 E+06	2.03 E+06	2.838 E+06	3.697 E+06	2.468 E+06
<i>Crack length=4.1 mm, third position</i>	<i>contour 2</i>	<i>contour 3</i>	<i>contour 4</i>	<i>contour 5</i>	<i>average</i>
JK	10.98	24.44	43.46	68.14	36.75
K_I(Pa√m)	1.606E+06	2.4E+06	2.195E+06	4 E+06	2.8 E+06
<i>Crack length=4.1 mm, fourth position</i>	<i>contour 2</i>	<i>contour 3</i>	<i>contour 4</i>	<i>contour 5</i>	<i>average</i>
JK	10.57	24.54	45.12	72.95	38.29
K_I(Pa√m)	1.576 E+06	2.4 E+06	3.255 E+06	4.139 E+06	2.843 E+06

It must be said that according to the table 8, the value of the stress intensity factor is increasing as the position comes near to the deepest point. Moreover, in a separate diagram, it will be shown that the value of stress intensity factor at the deepest point is greater than that at the corner point.

Table 9
Comparison of J-integral calculation and JK

<i>Crack length a=4.1 (mm)</i>	<i>Crack depth c(mm)</i>	<i>E(GPa)</i>	<i>K_I(MPa√m)</i>	<i>JK</i>	<i>J-integral</i>	<i>Error%</i>
first position	4	213.7	2.425	26.91	27.5181329	2.20
second position	4	213.7	2.468	29.33	28.502686	2.90
third position	4	213.7	2.8	36.75	36.6869443	1.71
fourth position	4	213.7	2.843	38.29	37.8224099	1.23

The same calculation has been done for a crack length of 4.2 mm. Table 11 indicates the accuracy of evaluation using finite elements analysis. Exception for this length, the error is not ignorable like other lengths. The reason for this may be related to model and partitions of software. But there is a good and acceptable accuracy for other lengths.

Table 10
Calculation of J-integral and stress intensity factor for a=4.2 mm by finite elements

<i>Crack length=4.2 mm, first position</i>	<i>contour 2</i>	<i>contour 3</i>	<i>contour 4</i>	<i>contour 5</i>	<i>average</i>
JK	9.631	19.07	31.01	45.1	26.21
K_I(Pa√m)	1.50E+06	2.12E+06	2.70E+06	3.26E+06	2.39E+06
<i>Crack length=4.2 mm, second position</i>	<i>contour 2</i>	<i>contour 3</i>	<i>contour 4</i>	<i>contour 5</i>	<i>average</i>
JK	7.081	16.96	33.08	56.16	28.32
K_I(Pa√m)	1.29E+06	2.00E+06	2.79E+06	3.63E+06	2.43E+06
<i>Crack length=4.2 mm, third position</i>	<i>contour 2</i>	<i>contour 3</i>	<i>contour 4</i>	<i>contour 5</i>	<i>average</i>
JK	10.75	23.82	42.28	66.27	35.78
K_I(Pa√m)	1.60E+06	2.37E+06	3.15E+06	3.95E+06	2.76E+06
<i>Crack length=4.2 mm, fourth position</i>	<i>contour 2</i>	<i>contour 3</i>	<i>contour 4</i>	<i>contour 5</i>	<i>average</i>
JK	10.35	23.91	43.88	70.88	37.25
K_I(Pa√m)	1.60E+06	2.37E+06	3.21E+06	4.08E+06	2.81E+06

Table.11
Comparison of J-integral calculations and JK

<i>Crack length a=4.2 (mm)</i>	<i>Crack depth c(mm)</i>	<i>E(GPa)</i>	<i>K_I(MPa√m)</i>	<i>JK</i>	<i>J-integral</i>	<i>Error%</i>
first position	4	213.7	2.39	26.21	26.72953	1.9436
second position	4	213.7	2.43	28.32	27.51813	2.914
third position	4	213.7	2.76	35.78	35.72377	1.574
fourth position	4	213.7	2.81	37.25	36.81809	1.1731

Crack length 4.3 mm is evaluated. The values are shown in table 12. Table 13 indicates the accuracy of evaluation using finite element analysis. The accuracy is very good.

Table 12
Calculation of J-integral and stress intensity factor for a=4.3 mm by finite elements

<i>crack length=4.3 mm, first position</i>	<i>contour 2</i>	<i>contour 3</i>	<i>contour 4</i>	<i>contour 5</i>	<i>average</i>
JK	9.327	17.65	27.92	39.81	18.94
K_I(Pa√m)	1.48E+06	2.04E+06	2.56E+06	3.06E+06	1.83E+06
<i>crack length=4.3 mm, second position</i>	<i>contour 2</i>	<i>contour 3</i>	<i>contour 4</i>	<i>contour 5</i>	<i>average</i>
JK	7.56	17.74	34.09	57.31	23.34
K_I(Pa√m)	1.33E+06	2.04E+06	2.83E+06	3.67E+06	1.97E+06
<i>crack length=4.3 mm, third position</i>	<i>contour 2</i>	<i>contour 3</i>	<i>contour 4</i>	<i>contour 5</i>	<i>average</i>
JK	9.731	19.98	33.6	50.31	27.72
K_I(Pa√m)	1.51E+06	2.17E+06	2.81E+06	3.44E+00	1.99E+06
<i>crack length=4.3 mm, fourth position</i>	<i>contour 2</i>	<i>contour 3</i>	<i>contour 4</i>	<i>contour 5</i>	<i>average</i>
JK	10.82	24.41	43.95	69.89	29.81
K_I(Pa√m)	1.59E+06	2.39E+06	3.21E+06	4.05E+06	2.25E+06

Table. 13
Comparison J-integral calculation and JK

<i>Crack length a=4.3 (mm)</i>	<i>Crack depth c(mm)</i>	<i>E(GPa)</i>	<i>K_I(MPa√m)</i>	<i>JK</i>	<i>J-integral</i>	<i>Error%</i>
first position	4	213.7	1.83	18.94	15.62	17.5
second position	4	213.7	1.97	23.34	18.23	21.2
third position	4	213.7	1.99	27.72	18.44	33.4
fourth position	4	213.7	2.25	29.81	23.69	20.5

Crack length 4.4 mm is evaluated. The values are shown in table 14. Table 15 indicates the accuracy of evaluation using finite element analysis. The accuracy is very good.

Table 14
Calculation of J-integral and stress intensity factor for a=4.4 mm by finite element

<i>Crack length=4.4 mm, first position</i>	<i>contour 2</i>	<i>contour 3</i>	<i>contour 4</i>	<i>contour 5</i>	<i>average</i>
JK	9.546	18.86	30.66	44.68	25.93
K_I(Pa√m)	1.50E+06	2.10E+06	2.6E+06	3.24E+06	2.37E+06
<i>Crack length=4.4 mm, second position</i>	<i>contour 2</i>	<i>contour 3</i>	<i>contour 4</i>	<i>contour 5</i>	<i>average</i>
JK	6.882	16.3	31.65	53.65	27.12
K_I(Pa√m)	1.27E+06	1.96E+06	2.73E+06	3.55E+06	2.38E+06
<i>Crack length=4.4 mm, third position</i>	<i>contour 2</i>	<i>contour 3</i>	<i>contour 4</i>	<i>contour 5</i>	<i>average</i>
JK	10.53	23.17	41.02	64.2	34.73
K_I(Pa√m)	1.57E+06	2.33E+06	3.10E+06	3.88E+06	2.72E+06
<i>Crack length=4.4 mm, fourth position</i>	<i>contour 2</i>	<i>contour 3</i>	<i>contour 4</i>	<i>contour 5</i>	<i>average</i>
JK	10.1	23.16	42.33	68.21	35.95
K_I(Pa√m)	1.54E+06	2.33E+06	3.15E+06	4.00E+06	2.76E+06

Table 15
Comparison of J-integral calculation and JK

<i>Crack length a=4.4 (mm)</i>	<i>Crack depth c(mm)</i>	<i>E(GPa)</i>	<i>K_I(MPa√m)</i>	<i>JK</i>	<i>J-integral</i>	<i>Error%</i>
first position	4	213.7	2.37	25.93	26.40	2.25
second position	4	213.7	2.38	27.12	26.42	2.6
third position	4	213.7	2.72	34.73	34.70	0.09
fourth position	4	213.7	2.76	35.95	35.56	1.6

Crack length 4.5 mm is evaluated. The values are shown in table 16. Table 17 indicates the accuracy of evaluation using finite element analysis. The accuracy is very good.

Table 16
Calculation of J-integral and stress intensity factor for a=4.5 mm by finite elements

<i>Crack length=4.5 mm , first position</i>	<i>contour 2</i>	<i>contour 3</i>	<i>contour 4</i>	<i>contour 5</i>	<i>average</i>
JK	6.6	15.8	30.02	48.52	25.2
K_I(Pa√m)	1.26E+06	1.94E+06	2.70E+06	3.51E+06	1.81E+06
<i>Crack length=4.5 mm, second position</i>	<i>contour 2</i>	<i>contour 3</i>	<i>contour 4</i>	<i>contour 5</i>	<i>average</i>
JK	9.5	18.71	30.4	44.31	25.73
K_I(Pa√m)	1.49E+06	2.10E+06	2.67E+06	3.23E+06	2.37E+06
<i>Crack length=4.5 mm, third position</i>	<i>contour 2</i>	<i>contour 3</i>	<i>contour 4</i>	<i>contour 5</i>	<i>average</i>
JK	10.44	22.89	40.46	63.26	34.26
K_I(Pa√m)	1.57E+06	2.32E+06	3.08E+06	3.85E+06	2.71E+06
<i>Crack length=4.5 mm, fourth position</i>	<i>contour 2</i>	<i>contour 3</i>	<i>contour 4</i>	<i>contour 5</i>	<i>average</i>
JK	10	22.86	41.68	67.06	35.4
K_I(Pa√m)	1.53E+06	2.32E+06	3.13E+06	3.97E+06	2.74E+06

Table 17
Comparison of J-integral calculation and JK

<i>Crack length a=4.5 (mm)</i>	<i>Crack depth c(mm)</i>	<i>E(GPa)</i>	<i>K_I(MPa√m)</i>	<i>JK</i>	<i>J-integral</i>	<i>Error%</i>
first position	4	213.7	1.81	25.2	15.34	42.28
second position	4	213.7	2.37	25.73	26.35	2.41
third position	4	213.7	2.71	34.26	34.24	0.059
fourth position	4	213.7	2.74	35.4	35.05	0.97

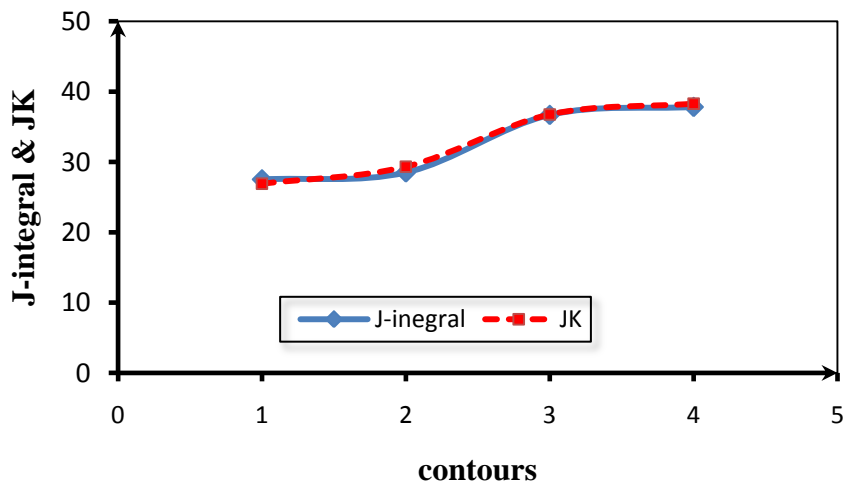


Figure 14
Accuracy of the J-integral, obtained from fracture mechanics analysis;
JK is calculated by finite elements, a=4.1 mm

For validation of results which obtained previously, the accuracy of contours are considered. For this purpose, JK and J-integral are compared in Figures below which indicate and confirm that there

is a good agreement between them. Also, stress intensity factor relates to the energy release rate. The stress intensity factor is calculated for the deepest point, $\varphi = 0^\circ$, and the corner point, $\varphi = 90^\circ$ and then compared with each other.

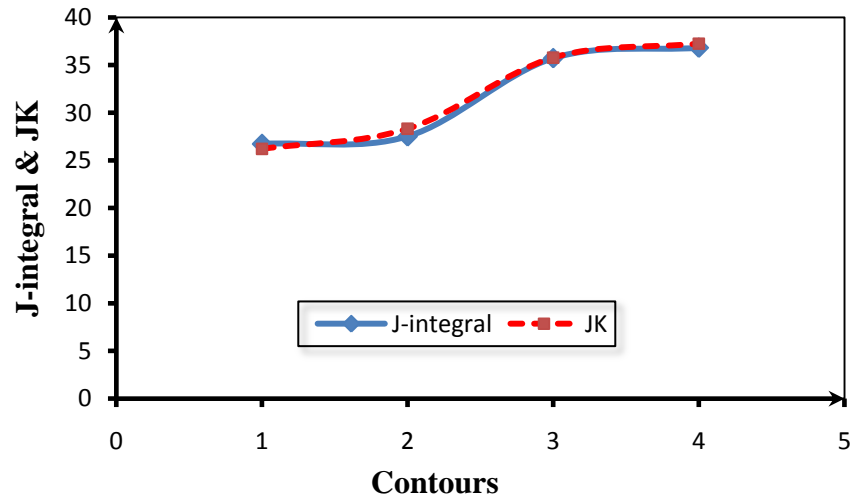


Figure 15

**Accuracy of the J-integral, obtained from fracture mechanics analysis;
JK is calculated by finite elements, a=4.2 mm**

Discussion

In the first step, comparison of JK method with the formula is commonly used in fracture mechanics is done. Finite element is employed to evaluate JK and in separated curves, the errors are illustrated and confirmed the especial accuracy between the values are obtained from fracture mechanics and the values are evaluated by finite element analysis. These curves are available in Fig. 14-18.

Obviously, the errors are ignorable and there is a good agreement between two methods but there is an exception related to crack length 4.3 mm. The two curves have considerable distance and not matched like other lengths. It may be because of the model and some hasty in evaluation but totally the results have good agreements.

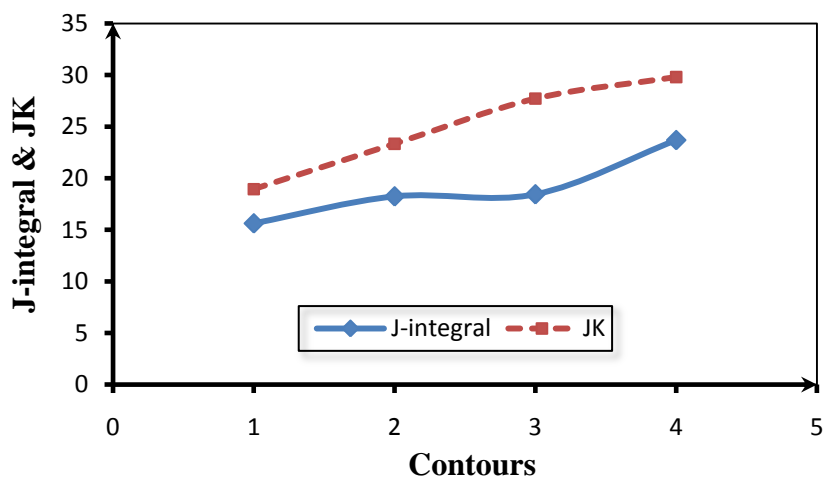


Figure 16

**Accuracy of the J-integral, obtained from fracture mechanics analysis;
JK is calculated by finite elements, a=4.3 mm**

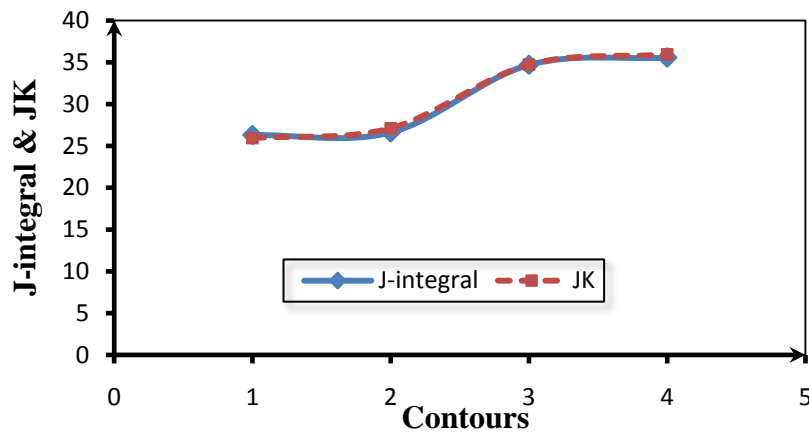


Figure 17

Accuracy of the J-integral, obtained from fracture mechanics analysis;
JK is calculated by finite elements, $a=4.4$ mm

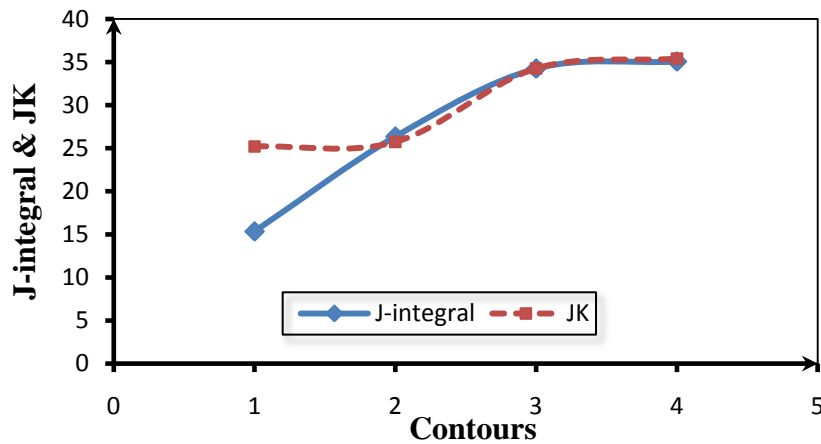


Figure 18

Accuracy of the J-integral, obtained from fracture mechanics analysis;
JK is calculated by finite elements, $a=4.5$ mm

Table 18

K_I for various positions and crack lengths at 34 MPa

Crack length (mm)	Crack depth (mm)	K_I corner point ($MPam^{0.5}$)	K_I deepest point ($MPam^{0.5}$)
5	5	18.4	19.84
6	6	18.9736	20.57062
7	7	20.7	21.72

In the second step, in table 18, K_I is calculated for different crack length. Moreover, Fig. 12 illustrates the position of deepest and corner points on half crack length. Also, a comparison between corner point stress and deepest point intensity factor is done and stress intensity factor as a function of the crack length is drawn and Fig. 19 shows these changes. In this case, because of having clear differences show the changes of stress intensity factor, the range of the crack lengths is changed from 4.1 to 4.5 into 5 to 7. In the past section, comparison between different methods of

calculating stress intensity factor in ABAQUS was evaluated and now, the changes stress intensity factor as a function of crack length are illustrated. Parameters in table 18 are evaluated for hydrogen pressure 34 MPa. Obviously, K_I is increasing as a crack length is growing. Fig. 19 illustrates these changes well.

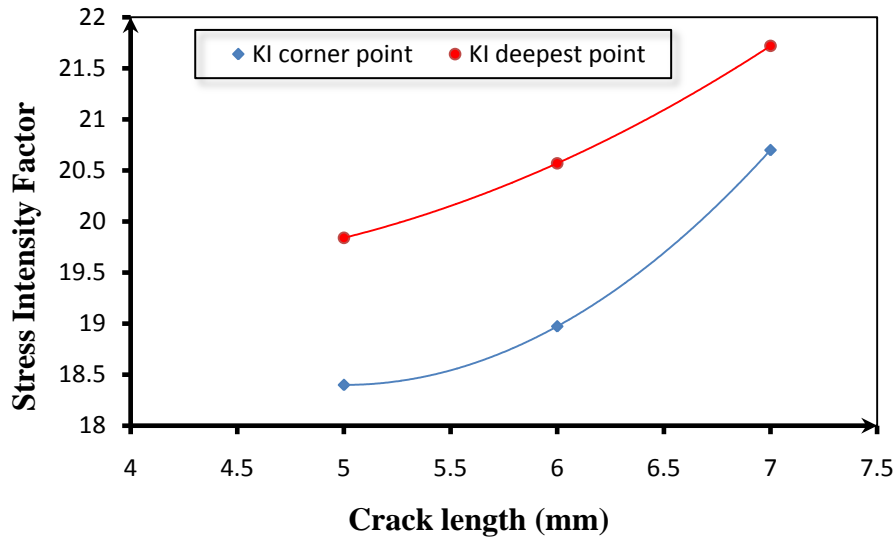


Figure 19
Changes in stress intensity factor as a function of crack length
for depth point and corner point of a crack

The value of K_I at the deepest point greater than that at the corner point, and Fig. 19 confirms this result. It is very common because the problem is solved in LEFM. The crack mouth tends to open when subjected to tension, so the boundary around it resistant against opening crack and this is more than resistance of boundary near the corner pint. In other words, the plastic zone around the corner point causes to decrease this limitation for opening the crack in this position. If there is a fatigue analysis and the crack exposes to a cyclic load, it is possible that the value for stress intensity in corner point is more than the deepest point. To calculate critical length, it is sufficient to evaluate the crack growth until to K_I is reaches to K_{IC} .

Conclusion

This study investigated contour integrals for axisymmetrical and LEFM model. As a result, J-integral which has closed relation to energy release associated with the crack growth increased the same as increasing of JK. Also, accuracy of using FEM method for calculating of stress intensity factor in different diagram confirmed that the model which was made in FEM was very prefect. On the other hand, the values of the J-integral are based on the stress intensity factors, JK, and by evaluating the contour integral directly, JA was shown a correlation between crack propagation and stress intensity factor for elliptic crack subjected to uniform tension that finite element analysis employed to model a pressure vessel with a blunting crack. Moreover, the stress intensity factor was developed based on elastic deformation concept. Besides, while the load was constant, stress intensity factor obtained for different length and position of crack front. As a result, the stress intensity factor in deepest point had greater value rather than the stress intensity in corner points for two reasons first; the resistance of the material against the crack propagation was stronger in the deepest point. Second, analysis was done for static loading in LEFM. In fatigue analysis, it is very common that the values of stress intensity factor in corner points are greater than the deepest point. The comparison of different values of stress intensity factor that calculated by finite element and by formula of standard in hand book showed a good agreement. Also, stress intensity evaluation is very important because the critical length of crack is estimated by reaching this value to the fracture toughness.

References

- [1] J. O'M. Bockris and P. K. Subramanyan, *A Thermodynamic Analysis of Hydrogen in Metals in the Presence of an Applied Stress Field*, Acta Metallurgica, **19** (1971) 1205
- [2] M.A. Guerrero a, C. Betegon, J. Belzunce, *Fracture Analysis of a Pressure Vessel Made of High Strength Steel (HSS)*, Engineering Failure Analysis, article in press, 2007.
- [3] A. T. Yokobori, JR, T. Nemoto, K. Satoh, and T. Yamada, *Numerical Analysis of Hydrogen Diffusion and Concentration in Solid with Emission around the Crack Tip*, Engineering Fracture Mechanics, **55**[1] (1996) 47-60, G. Muller, M. Uhlemann, A. Ulbricht, J. Bohmert, *Influence of Hydrogen on Toughness of Irradiated Reactor Pressure Vessel Steels*, Journal of Nuclear Materials, **359** (2006) 114-121
- [4] J Ulrich Krupp, *Fatigue Crack Propagation in Metals and Alloys: Microstructure Aspects and Modeling Concepts*, WILEY-VCH Verlag GmbH & Co. KGaA, Germany, 2007
- [5] Douglas M. Symons, *A Comparison of Internal Hydrogen Embrittlement and Hydrogen Environment Embrittlement of X-750*, Eng. Fracture Mech. **68** (2001) 751-771
- [6] C. J. McMahon Jr., *Hydrogen-Induced Intergranular Fracture of Steels*, Eng. Fracture, Mech., **68** (2001) 773-788
- [7] J. M. Smith and H. C. Van Ness, *Introduction to Chemical Engineering Thermodynamics*, McGraw-Hill, International edition, fourth edition, New York (1916)
- [8] J. M. Prausnitz, R. N. Lichtenthaler, E. G. de Azevedo, *Molecular Thermodynamics of Fluid-Phase Equilibrium*, 3rd Edition, Prentice Hall International Series in Physical and Chem. Eng. Sci., New York (1998)
- [9] C. R. Aronachalam, *Hydrogen Charging and Internal Hydrogen Effects on Interfacial and Fracture Properties of Metal Matrix Composites*, submitted by Michigan University, James places, Department of Material Science and Mechanics (1994)
- [10] M. R. Louthan, Jr., *Hydrogen Embrittlement of Metals: a Primer for the Failure Analyst*, Materials Science and Technology, J. of Failure Analysis and Prevention, **8** (2008) 289-307
- [11] H. P. Van Leeuwen, *The Kinetics of Hydrogen Embrittlement: a Quantitative Diffusion Model*, Eng. Fracture Mech., **6** (1974) 141-161
- [12] J. Toribio, *The Role of Crack Tip Strain Rate in Hydrogen Assisted Cracking*, Corr. Sci., **39** (1997) 1687-1697
- [13] Y. Kim, Y. J. Chao, Marty J. Pechersky and Michael J. Morgan, *On the Effect of Hydrogen on Fracture Toughness of Steel*, Int. J. of Fracture, **134** (2005) 339-347
- [14] J. O'M. Bockris and P. K. Subramanyan, *A Thermodynamic Analysis of Hydrogen in Metals in the Presence of an Applied Stress Field*, Acta Metall., **19** (1971) 1205
- [15] H. P. Van Leeuwen, *A Failure Criterion for Internal Hydrogen Embrittlement*, Fracture Mech., **9** (1997) 291-296
- [16] Bong-Sang Lee, Min-Chul Kim, Maan-Won Kim, Ji-Hyun Yoon, Jun-Hwa Hong, *Master Curve Techniques to Evaluate Irradiation Embrittlement of Nuclear Reactor Pressure Vessels for Long-Term Operation*, Int. J. of Pressure Vessel and Piping, **85** (2008) 593-599
- [17] George Karzov, Boris Margolin, Eugene Rivkin, *Analysis of Structure Integrity of RPV on the Basis of Brittle Criterion: New Approaches*, Int. J. of Pressure Vessel and Piping, **81** (2004) 651-656

-
- [18] A. Toshimitsu Yokobori Jr., Yasrou Chida, Takenao Nemoto, Kogi Satoh, Tetsuya Yamada, *The Characteristics of Hydrogen Diffusion and Concentration around a Crack Tip Concerned with Hydrogen Embrittlement*, *Corr. Sci.*, **44** (2001) 407-424
- [19] A. T. Yokobori, JR, T. Nemoto, K. Satoh, and T. Yamada, *Numerical Analysis of Hydrogen Diffusion and Concentration in Solid with Emission around the Crack Tip*, *Eng. Fracture Mech.*, **55** (1996) 47-60
- [20] J. O'M. Bockris and P. K. Subramanyan, *A Thermodynamic Analysis of Hydrogen in Metals in the Presence of an Applied Stress Field*, *Acta Metal.*, **19** (1971) 1205
- [21] Hirokazu Kotake, Royosuke Matsumoto, Shinya Taketomi, Noriyuke Miyazaki, *Transient Hydrogen Diffusion Analyses Coupled with Crack-Tip Plasticity under Cyclic Loading*, *Int. J. of Pressure Vessel and Piping*, **85** (2008) 540-549
- [22] Murakami, Y., *The Handbook of Stress Intensity Factors*, Pergamon (Oxford, New York), 1987

Defects and Diffusion in Semiconductors XII

10.4028/www.scientific.net/DDF.303-304

Analysis of Stress Intensity Factor and Crack Propagation for Alloy X-750 Pressure Vessel with a Blunting Crack

10.4028/www.scientific.net/DDF.303-304.63

DOI References

- [5] Douglas M. Symons, A Comparison of Internal Hydrogen Embrittlement and Hydrogen Environment Embrittlement of X-750, Eng. Fracture Mech. 68 (2001) 751-771
doi:10.1016/S0013-7944(00)00123-5
- [12] J. Toribio, The Role of Crack Tip Strain Rate in Hydrogen Assisted Cracking, Corr. Sci., 39 (1997) 1687-1697
doi:10.1016/S0010-938X(97)00075-9
- [13] Y. Kim, Y. J. Chao, Marty J. Pechersky and Michael J. Morgan, On the Effect of Hydrogen on Fracture Toughness of Steel, Int. J. of Fracture, 134 (2005) 339-347
doi:10.1007/s10704-005-1974-7
- [16] Bong-Sang Lee, Min-Chul Kim, Maan-Won Kim, Ji-Hyun Yoon, Jun-Hwa Hong, Master Curve Techniques to Evaluate Irradiation Embrittlement of Nuclear Reactor Pressure Vessels or Long-Term Operation, Int. J. of Pressure Vessel and Piping, 85 (2008) 593-599
doi:10.1016/j.ijpvp.2007.08.005
- [17] George Karzov, Boris Margolin, Eugene Rivkin, Analysis of Structure Integrity of RPV on the Basis of Brittle Criterion: New Approaches, Int. J. of Pressure Vessel and Piping, 81 (2004) 51-656
doi:10.1016/j.ijpvp.2004.03.001
- [1] J. O'M. Bockris and P. K. Subramanyan, A Thermodynamic Analysis of Hydrogen in Metals in the Presence of an Applied Stress Field, Acta Metallurgica, 19 (1971) 1205
doi:10.1016/0001-6160(71)90053-8
- [5] Douglas M. Symons, A Comparison of Internal Hydrogen Embrittlement and Hydrogen Environment Embrittlement of X-750, Eng. Fracture Mech. 68 (2001) 751-771
doi:10.1016/S0013-7944(00)00123-5
- [6] C. J. McMahon Jr., Hydrogen-Induced Intergranular Fracture of Steels, Eng. Fracture, Mech., 68 (2001) 773-788
doi:10.1016/S0013-7944(00)00124-7
- [10] M. R. Louthan, Jr., Hydrogen Embrittlement of Metals: a Primer for the Failure Analyst, Materials Science and Technology, J. of Failure Analysis and Prevention, 8 (2008) 289-307
doi:10.1007/s11668-008-9133-x
- [12] J. Toribio, The Role of Crack Tip Strain Rate in Hydrogen Assisted Cracking, Corr. Sci., 39 (1997) 1687-1697
doi:10.1016/S0010-938X(97)00075-9
- [13] Y. Kim, Y. J. Chao, Marty J. Pechersky and Michael J. Morgan, On the Effect of Hydrogen on Fracture Toughness of Steel, Int. J. of Fracture, 134 (2005) 339-347
doi:10.1007/s10704-005-1974-7
- [14] J. O'M. Bockris and P. K. Subramanyan, A Thermodynamic Analysis of Hydrogen in Metals in the Presence of an Applied Stress Field, Acta Metall., 19 (1971) 1205
doi:10.1016/0001-6160(71)90053-8

- [16] Bong-Sang Lee, Min-Chul Kim, Maan-Won Kim, Ji-Hyun Yoon, Jun-Hwa Hong, Master Curve Techniques to Evaluate Irradiation Embrittlement of Nuclear Reactor Pressure Vessels for Long-Term Operation, *Int. J. of Pressure Vessel and Piping*, 85 (2008) 593-599
doi:10.1016/j.ijpvp.2007.08.005
- [17] George Karzov, Boris Margolin, Eugene Rivkin, Analysis of Structure Integrity of RPV on the Basis of Brittle Criterion: New Approaches, *Int. J. of Pressure Vessel and Piping*, 81 (2004) 651-656
doi:10.1016/j.ijpvp.2004.03.001
- [19] A. T. Yokobori, JR, T. Nemoto, K. Satoh, and T. Yamada, Numerical Analysis of Hydrogen Diffusion and Concentration in Solid with Emission around the Crack Tip, *Eng. Fracture Mech.*, 55 (1996) 47-60
doi:10.1016/0013-7944(96)00002-1
- [20] J. O'M. Bockris and P. K. Subramanyan, A Thermodynamic Analysis of Hydrogen in Metals in the Presence of an Applied Stress Field, *Acta Metal.*, 19 (1971) 1205
doi:10.1016/0001-6160(71)90053-8